

Stochastic resonance in bistable systems with nonlinear dissipation and multiplicative noise: A microscopic approach

Hideo Hasegawa*

Department of Physics, Tokyo Gakugei University, Koganei, Tokyo 184-8501, Japan

(Dated: March 11, 2019)

Abstract

The stochastic resonance (SR) in bistable systems has been extensively discussed with the use of *phenomenological* Langevin models. In this paper, we study SR of an open bistable system subjected to a bath coupled with a nonlinear system-bath interaction, which is described by the *microscopic*, generalized Caldeira-Leggett (CL) model. The adopted CL model yields the non-Markovian Langevin equation with nonlinear dissipation and state-dependent diffusion which preserve the fluctuation-dissipation relation (FDR). Our numerical calculations show that (1) the stationary probability distribution function is independent of noise parameters of a , b and τ although the spectral power amplification (SPA) depends on them where a (b) denotes the magnitude of multiplicative (additive) noise and τ expresses the relaxation time of colored noise, (2) the SPA exhibits SR not only for a and b but also for τ , and (3) the SPA for coexisting additive and multiplicative noises has a single-peak but two-peak structure as functions of a , b and/or τ . These results (1)-(3) are in contrast with previous ones obtained by the universal colored-noise approximation applied to phenomenological Langevin models where the FDR is not held.

PACS numbers: 05.70.-a, 05.40.-a, 05.10.Gg

*hideohasegawa@goo.jp

I. INTRODUCTION

In the last three decades since a seminal work of Benzi *et. al.* [1], extensive studies have been made on the stochastic resonance (SR) which shows a beneficial role of noise (for a recent review on SR, see Refs. [2, 3]). Initial studies on SR were made with the use of a two-state model and the Langevin model subjected to white noise given by

$$\dot{x} = -V'(x) + \xi(t) + f(t), \quad (1)$$

where $V(x)$ expresses the bistable potential, dot and prime stand for derivatives with respect to time and argument, respectively, $f(t)$ denotes an external input (force), $\xi(t)$ is zero-mean Gaussian noise with $\langle \xi(t)\xi(t') \rangle = 2D\delta(t - t')$, and D is the strength of white noise. It has been shown that the signal-to-noise ratio (SNR) for a periodic input exhibits the maximum when D is changed, which signifies an enhanced transmission for an optimum magnitude of noise. Subsequent studies on SR examined effects of colored noise given by $\langle \xi(t)\xi(t') \rangle = (D/\tau)e^{-|t-t'|/\tau}$ in Eq. (1) [4–7]: in the limit of $\tau \rightarrow 0$, colored noise tends to white noise (for a review on colored noise, see Ref. [8]). Calculations using the universal colored-noise approximation (UCNA) [9] have shown that noise color suppresses SR monotonically with the relaxation time τ [4–7]. In recent years, studies on SR have been made with the use of the Langevin model subjected to more sophisticated noise [10–12], in which the generalized Langevin model includes correlated additive white noise and multiplicative colored noise given by

$$\dot{x} = -V'(x) + \xi(t) + G(x)\eta(t) + f(t). \quad (2)$$

Here $G(x)$ is a function of x , $\xi(t)$ and $\eta(t)$ stand for zero-mean white and colored noises, respectively, with correlations: $\langle \xi(t)\xi(t') \rangle = 2D\delta(t - t')$, $\langle \eta(t)\eta(t') \rangle = (M/\tau) e^{-|t-t'|/\tau}$ and $\langle \xi(t)\eta(t') \rangle = 2\lambda\sqrt{DM}$; M and τ denote the magnitude and relaxation time of multiplicative colored noises, and λ is the coupling strength between additive and multiplicative noises. SNR of the generalized Langevin model calculated by using the UCNA and the functional-integral method shows a complicated behavior as functions of D , M and λ : for example, the SNR may have the bimodal structure when these parameters are varied [10, 11]. Ref. [12] studied effects of the finite relaxation time τ_c in the coupling between additive white noise and multiplicative colored noise given by $\langle \xi(t)\eta(t') \rangle = (\lambda\sqrt{DM}/\tau_c) e^{-|t-t'|/\tau_c}$ in Eq. (2).

Equations (1) and (2) express the overdamped Langevin models, while their underdamped (Markovian) counterparts are given by

$$\ddot{x} = -V'(x) - \gamma_0 \dot{x} + \xi(t) + f(t), \quad (3)$$

$$\ddot{x} = -V'(x) - \gamma_0 \dot{x} + \xi(t) + G(x)\eta(t) + f(t), \quad (4)$$

where γ_0 denotes a friction coefficient. The overdamped Langevin models given by Eqs. (1) and (2) may be derived by an appropriate elimination of \ddot{x} terms in Eqs. (3) and (4), respectively. Dissipation and diffusion terms in Eq. (3) satisfy the second-kind fluctuation-dissipation relation (FDR),

$$D = k_B T \gamma_0, \quad (5)$$

where k_B is the Boltzmann constant and T denotes the temperature. The FDR implies that dissipation and diffusion processes originate from the same event. It is noted that (a) the phenomenological Langevin models given by Eqs. (2) and (4) have no microscopic bases, (b) the FDR in Eqs. (2) and (4) is not definite, and (c) the finite correlation time τ of colored noise $\eta(t)$ is not consistent with the local dissipative term of γ_0 in Eq. (4). The importance of going beyond the deficits (a)-(c) has been recognized over many decades. The microscopic origin of additive noise has been proposed within a framework of Caldeira-Leggett (CL) system-bath Hamiltonian [13–15]. The CL model with a linear system-bath coupling leads to the non-Markovian Langevin equation expressed by [13–15]

$$\ddot{x} = -V'(x) - \int_{-\infty}^t \gamma(t-t') \dot{x}(t') dt' + \xi(t), \quad (6)$$

where the dissipation kernel $\gamma(t-t')$ and additive noise $\xi(t)$ are expressed in terms of bath variables and they satisfy the FDR,

$$\langle \xi(t)\xi(t') \rangle = k_B T \gamma(t-t'). \quad (7)$$

By using the generalized CL model including a nonlinear system-bath coupling, we may obtain the non-Markovian Langevin equation with multiplicative noise which preserves the FDR [see Eq. (14)] [16, 17]. The nature of nonlinear dissipation and multiplicative noise has been recently explored with renewed interest [18–20]. Nonlinear dissipation and multiplicative noise have been recognized as important ingredients in several fields such as mesoscopic

scale systems [21, 22] and ratchet problems [23–26]. Quite recently, we have studied the generalized CL model for a harmonic oscillator which includes non-linear non-local dissipation and multiplicative diffusion [27]. It has been shown that the stationary probability distribution function (PDF) is independent of magnitudes of additive and multiplicative noises and the relaxation time of colored noise [18–20, 27] although the average response to applied input depends on noise parameters [27]. This is in contrast with previous studies which show that the stationary PDF of the Langevin model for $V'(x) = x$ with $\tau = \lambda = 0$ in Eq. (2) is Gaussian or non-Gaussian, depending on D and M [28–30]. We suppose that when the generalized CL model with a nonlinear coupling [18–20, 27] is applied to a bistable system, properties of the calculated SR may be rather different from those having been derived by the phenomenological Langevin model given by Eq. (2) or (4) [4–8, 10–12].

It is the purpose the present paper to make a detailed study of SR of an open bistable system described by the generalized CL model with nonlinear nonlocal dissipation and state-dependent diffusion [27]. Although the UCNA has been employed in many studies on SR for colored noise [4, 5, 10–12] because it is exact both for $\tau = 0.0$ and $\tau = \infty$, its validity within $O(\tau)$ is not justified [31, 32]. In this study, we have investigated SR for a wide range of τ value by using simulations. Such a calculation has not been reported as far as we are aware of.

The paper is organized as follows. In the following Sec. II, we briefly summarize the non-Markovian Langevin equation derived from the generalized CL model with the Ornstein-Uhlenbeck (OU) process for colored noise [18–20, 27]. In Sec. III, after studying the stationary PDF, we investigate SR of an open bistable system for three cases: additive noise only, multiplicative noise only, and coexisting additive and multiplicative noises. In Sec. IV, we discuss the overdamped limit of the Markovian Langevin model subjected to multiplicative noise and the CL-type model including two kinds of noise. Sec. V is devoted to our conclusion.

II. THE GENERALIZED CL MODEL

A. Non-Markovian Langevin equation

We consider a system of a Brownian particle coupled to a bath consisting of N -body uncoupled oscillators, which is described by the generalized CL model [18–20, 27],

$$H = H_S + H_B + H_I, \quad (8)$$

with

$$H_S = \frac{p^2}{2} + V(x) - xf(t), \quad (9)$$

$$H_B + H_I = \sum_{n=1}^N \left\{ \frac{p_n^2}{2m_n} + \frac{m_n \omega_n^2}{2} \left(q_n - \frac{c_n \phi(x)}{m_n \omega_n^2} \right)^2 \right\}. \quad (10)$$

Here H_S , H_B and H_I express Hamiltonians of the system, bath and interaction, respectively; x , p and $V(x)$ denote position, momentum and potential, respectively, of the system; q_n , p_n , m_n and ω_n stand for position, momentum, mass and frequency, respectively, of bath; the system couples to the bath nonlinearly through a function $\phi(x)$; $f(t)$ expresses an applied external force. The original CL model adopts a linear system-bath coupling with $\phi(x) = x$ in Eq. (10) which yields additive noise [15]. By using the standard procedure, we obtain the generalized Langevin equation given by [15–18, 27]

$$\ddot{x}(t) = -V'(x(t)) - \phi'(x(t)) \int_0^t \gamma(t-t') \phi'(x(t')) \dot{x}(t') dt' + \phi'(x(t)) \zeta(t) + f(t), \quad (11)$$

with

$$\gamma(t) = \sum_{n=1}^N \left(\frac{c_n^2}{m_n \omega_n^2} \right) \cos \omega_n t, \quad (12)$$

$$\zeta(t) = \sum_{n=1}^N \left\{ \left[\frac{m_n \omega_n^2}{c_n} q_n(0) - \phi(x(0)) \right] \left(\frac{c_n^2}{m_n \omega_n^2} \right) \cos \omega_n t + \left(\frac{c_n p_n(0)}{m_n \omega_n} \right) \sin \omega_n t \right\}, \quad (13)$$

where $\gamma(t-t')$ denotes the non-local kernel and $\zeta(t)$ stands for noise. Dissipation and diffusion terms given by Eqs. (12) and (13), respectively, satisfy the FDR,

$$\langle \zeta(t) \zeta(t') \rangle_0 = k_B T \gamma(t-t'), \quad (14)$$

where the bracket $\langle \cdot \rangle_0$ stands for the average over initial states of $q_n(0)$ and $p_n(0)$ [16–18].

We adopt the OU process for the kernel $\gamma(t-t')$ given by

$$\gamma(t-t') = \left(\frac{\gamma_0}{\tau}\right) e^{-(t-t')/\tau}, \quad (15)$$

where γ_0 and τ stand for the strength and relaxation time, respectively, of colored noise.

The OU colored noise may be generated by the differential equation,

$$\dot{\zeta}(t) = -\frac{\zeta(t)}{\tau} + \frac{\sqrt{2k_B T \gamma_0}}{\tau} \xi(t), \quad (16)$$

where $\xi(t)$ expresses white noise with

$$\langle \xi(t) \rangle = 0, \quad \langle \xi(t)\xi(t') \rangle = \delta(t-t'). \quad (17)$$

Equations (16) and (17) lead to the PDF and correlation of colored noise given by

$$P(\zeta) \propto e^{-(\beta\tau/2\gamma_0)\zeta^2}, \quad (18)$$

$$\langle \zeta(t)\zeta(t') \rangle = \left(\frac{k_B T \gamma_0}{\tau}\right) e^{-(t-t')/\tau} = k_B T \gamma(t-t'), \quad (19)$$

where $\beta = 1/k_B T$.

In order to transform the non-Markovian Langevin equation given by Eq. (11) into more tractable multiple differential equations, we introduce a new variable $u(t)$ [17, 20],

$$u(t) = -\int_0^t \gamma(t-t')\phi'(x(t'))\dot{x}(t') dt', \quad (20)$$

which yields four first-order differential equations for $x(t)$, $p(t)$, $u(t)$ and $\zeta(t)$ given by

$$\dot{x}(t) = p(t), \quad (21)$$

$$\dot{p}(t) = -V'(x) + \phi'(x(t))u(t) + f(t) + \phi'(x(t))\zeta(t), \quad (22)$$

$$\dot{u}(t) = -\frac{u(t)}{\tau} - \left(\frac{\gamma_0}{\tau}\right)\phi'(x(t))p(t), \quad (23)$$

$$\dot{\zeta}(t) = -\frac{\zeta(t)}{\tau} + \frac{\sqrt{2k_B T \gamma_0}}{\tau}\xi(t). \quad (24)$$

From Eqs. (21)-(24), we obtain the multi-variate Fokker-Planck equation (FPE) for distribution of $P(x, p, u, \zeta, t)$,

$$\begin{aligned} \frac{\partial P(x, p, u, \zeta, t)}{\partial t} &= -\frac{\partial}{\partial x} p P(x, p, u, \zeta, t) \\ &\quad - \frac{\partial}{\partial p} [-V'(x) + f(t) + \phi'(x)u + \phi'(x)\zeta] P(x, p, u, \zeta, t) \\ &\quad - \frac{\partial}{\partial u} \left[\frac{u}{\tau} + \left(\frac{\gamma_0}{\tau}\right)\phi'(x)p \right] P(x, p, u, \zeta, t) + \frac{\partial}{\partial \zeta} \left(\frac{\zeta}{\tau} \right) P(x, p, u, \zeta, t) \\ &\quad + \left(\frac{k_B T \gamma_0}{\tau^2} \right) \frac{\partial^2}{\partial \zeta^2} P(x, p, u, \zeta, t). \end{aligned} \quad (25)$$

The stationary PDF with $f(t) = 0$ is given by [17]

$$P(x, p) = \int P(x, p, u, \zeta) du d\zeta \propto e^{-\beta[p^2/2+V(x)]}. \quad (26)$$

B. Markovian Langevin equation

It is worthwhile to examine the local limit of Eq. (11) with a kernel $\gamma(t - t')$ given by

$$\gamma(t - t') = 2\gamma_0 \delta(t - t'), \quad (27)$$

which leads to the Markovian Langevin equation,

$$\ddot{x}(t) = -V'(x(t)) - \gamma_0 \phi'(x(t))^2 \dot{x}(t) + \sqrt{2k_B T \gamma_0} \phi'(x(t)) \xi(t) + f(t). \quad (28)$$

It is evident that the Markovian Langevin equation becomes a good approximation of the non-Markovian one in the limit of $\tau \rightarrow 0$.

From Eq. (28), we obtain first-order differential equations,

$$\dot{x}(t) = p(t), \quad (29)$$

$$\dot{p}(t) = -V'(x) - \gamma_0 \phi'(x(t))^2 p(t) + \sqrt{2k_B T \gamma_0} \phi'(x(t)) \xi(t) + f(t). \quad (30)$$

The relevant FPE for the PDF of $P(x, p, t)$ is expressed by

$$\begin{aligned} \frac{\partial P(x, p, t)}{\partial t} &= -\frac{\partial}{\partial x} p P(x, p, t) + \frac{\partial}{\partial p} [V'(x) - f(t) + \gamma_0 \phi'(x)^2 p] P(x, p, t) \\ &+ k_B T \gamma_0 \frac{\partial}{\partial p} \phi'(x) \frac{\partial}{\partial p} \phi'(x) P(x, p, t). \end{aligned} \quad (31)$$

The stationary distribution of Eq. (31) with $f(t) = 0$ is given by

$$P(x, p) \propto e^{-\beta[p^2/2+V(x)]}, \quad (32)$$

which is consistent with the result of the non-Markovian Langevin equation given by Eq. (26).

III. BISTABLE SYSTEMS

A. Stationary PDF

We apply the generalized CL model mentioned in the preceding section to a bistable system, where $V(x)$ and $\phi(x)$ in Eqs. (8)-(10) are given by

$$V(x) = \frac{x^4}{4} - \frac{x^2}{2}, \quad (33)$$

$$\phi(x) = \frac{ax^2}{2} + bx \quad (a \geq 0, b \geq 0), \quad (34)$$

a and b denoting magnitudes of multiplicative and additive noises, respectively. The symmetric bistable potential given by Eq. (33) has two stable minima at $x = \pm 1.0$ and unstable maximum at $x = 0.0$. The height of the potential barrier is given by $\Delta \equiv V(0) - V(\pm 1) = 1/4$.

First we show calculations of the stationary PDF. We have solved Eqs. (21)-(24) by using the Heun method [33, 34] with a time step of 0.001 for parameters of $\gamma_0 = 1.0$ and $k_B T = \Delta = 0.25$. Simulations of Eqs. (21)-(24) have been performed for $0 \leq t < 1000.0$ with discarding initial results at $t < 200.0$. Calculated results to be reported are averaged over 10 000 runs with initial states of Gaussian-distributed $x(0)$ and $p(0)$ with $\langle x(0) \rangle = \langle p(0) \rangle = 0$ and $\langle x(0)^2 \rangle = \langle p(0)^2 \rangle = k_B T$. Initial conditions of $u(0) = 0$ and $\zeta(0) = 0$ have been used in all simulations.

Calculated marginal PDFs of $P(x)$, $P(p)$, $P(u)$ and $P(\zeta)$ for $f(t) = 0$ are shown in Figs. 1(a), (b), (c) and (d), respectively, where four sets of parameters are adopted: $(a, b, \tau) = (1, 0, 10.0)$ (solid curves), $(1, 0, 0.1)$ (dashed curves), $(0, 1, 10.0)$ (chain curves) and $(0, 1, 0.1)$ (dotted curves). We note that $P(x)$ and $P(p)$ in Figs. 1(a) and (b) are independent of the parameters of (a, b, τ) although $P(u)$ and $P(\zeta)$ in Figs. 1(c) and (d) depend on them. Calculated $P(x)$ and $P(p)$ are in good agreement with marginal PDFs obtained by

$$P(x) = \int P(x, p) dp \propto e^{-\beta V(x)}, \quad (35)$$

$$P(p) = \int P(x, p) dx \propto e^{-\beta p^2/2}, \quad (36)$$

which show that $P(x)$ has the typical bimodal structure while $P(p)$ is Gaussian. Equation (18) shows that $P(\zeta)$ is the Gaussian PDF whose variance depends on τ for fixed γ_0 and T . In contrast, Fig. 1(c) shows that $P(u)$ is Gaussian PDF for additive noise but non-Gaussian

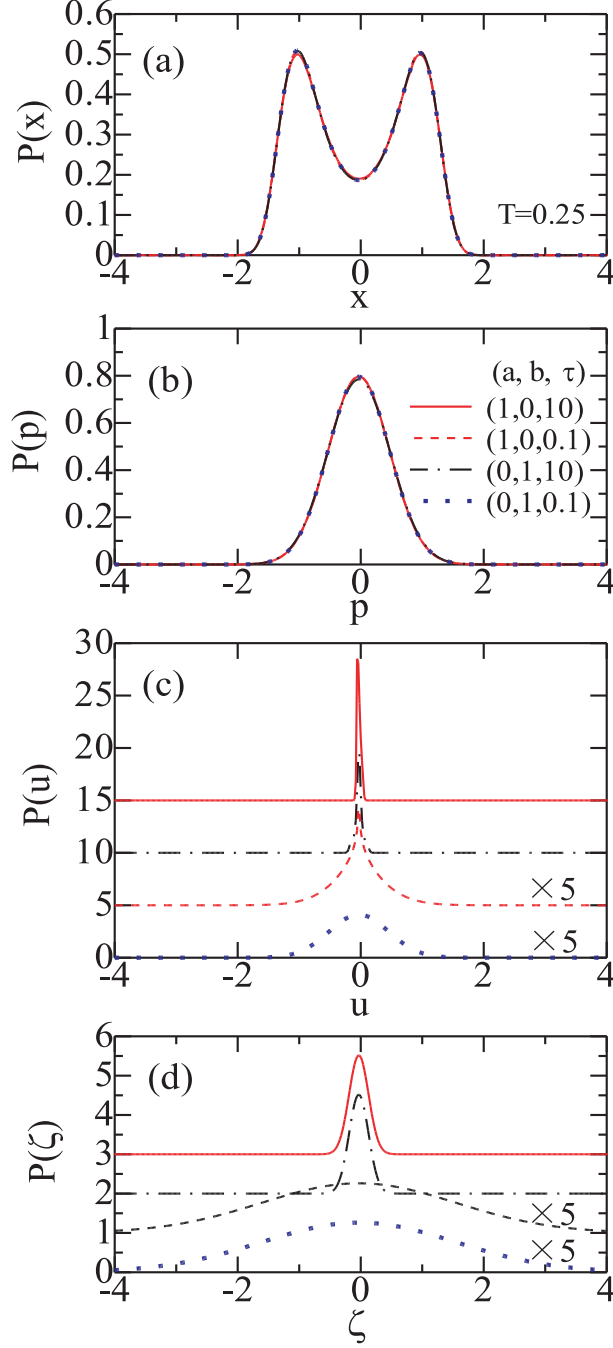


FIG. 1: (Color online) Marginal PDFs of (a) $P(x)$, (b) $P(p)$, (c) $P(u)$ and (d) $P(\zeta)$ for $(a, b, \tau) = (1, 0, 10.0)$ (solid curves), $(1, 0, 0.1)$ (dashed curves), $(0, 1, 10.0)$ (chain curves), and $(0, 1, 0.1)$ (dotted curves) calculated by simulations with $\gamma_0 = 1.0$ and $k_B T = \Delta = 0.25$. $P(x)$ and $P(p)$ in (a) and (b) are indistinguishable among the four sets of (a, b, τ) . $P(u)$ and $P(\zeta)$ for $(a, b, \tau) = (1, 0, 0.1)$ and $(0, 1, 0.1)$ are multiplied by a factor of five in (c) and (d) where PDFs are arbitrarily shifted for a clarity of figures.

PDF for multiplicative noise. Properties of stationary PDFs for bistable potential shown in Fig. 1 are similar to those for harmonic oscillators except for $P(x)$ (see Fig. 1 of Ref. [27]).

B. Stochastic resonance

1. Spectral power amplification

We investigate SR, applying a sinusoidal input given by

$$f(t) = g \cos\left(\frac{2\pi t}{T_0}\right) = g \cos \omega_0 t, \quad (37)$$

where g , T_0 and ω_0 ($= 2\pi/T_0$) denote its magnitude, period and frequency, respectively. A sinusoidal input given by Eq. (37) yields an averaged output given by

$$\mu(t) = \langle x(t) \rangle, \quad (38)$$

where $\langle \cdot \rangle$ denotes the average over trials. We evaluate the spectral power amplification (SPA) S defined by

$$S = \frac{|\mu[\omega_0]|^2}{|f[\omega_0]|^2}, \quad (39)$$

where $f[\omega]$ and $\mu[\omega]$ are Fourier transformations of $f(t)$ and $\mu(t)$, respectively. We have made direct simulations, solving Eqs. (21)-(24) with a small magnitude of $g = 0.05$ and $T_0 = 10.0$ in Eq. (37). Simulation procedures are the same as those for a calculation of stationary PDFs except for initial conditions of $x(0)$ and $p(0)$ which are taken to be $x(0) = 1.0$ and $p(0) = 0.0$.

2. Case of additive colored noise only

First we apply only additive colored noise ($a = 0.0$) to the system. Figure 2(a) shows SPA as a function of b for $\tau = 0.1$ (dashed curve), $\tau = 5.0$ (solid curve) and $\tau = 10.0$ (dashed curve). With increasing τ , the b value where S has the maximum is increased, and the maximum value of S (S_{max}) is gradually decreased with the wider distribution of S . Figure 2(b) shows the τ dependence of S calculated for $b = 0.2$ (dashed curve), $b = 0.4$ (solid curve) and $b = 0.6$ (dashed curve). S_{max} in Figs. 2(a) and 2(b) is observed at a larger b for a larger τ and vice versa.

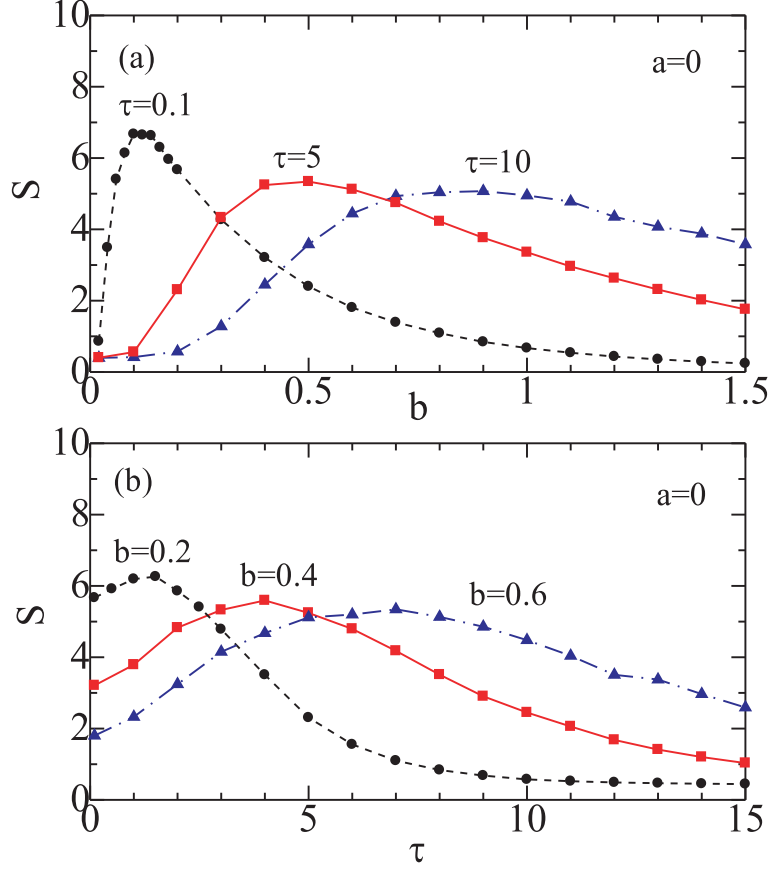


FIG. 2: (Color online) (a) SPA S for additive colored noise only as a function of b with $\tau = 0.1$ (dashed curve), $\tau = 5.0$ (solid curve) and $\tau = 10.0$ (chain curve). (b) S as a function of τ with $b = 0.2$ (dashed curve), $b = 0.4$ (solid curve) and $b = 0.6$ (chain curve) ($a = 0.0$, $g = 0.05$ and $T_0 = 10.0$).

Figure 3(a) shows a schematic plot of S as functions of b and τ , which is estimated from simulation results shown in Figs. 2(a) and 2(b). We note that with increasing b or τ , a location of S_{max} departs from the origin of $(b, \tau) = (0.0, 0.0)$ and its magnitude is gradually decreased. Circles in Fig. 3(b) denote locations of S_{max} in the b - τ plane obtained by simulations shown in Figs. 2(a) and (b). S_{max} nearly locates along the chain curve expressed by $b = 0.075\tau + 0.1$. Fig. 3(c) will be explained shortly.

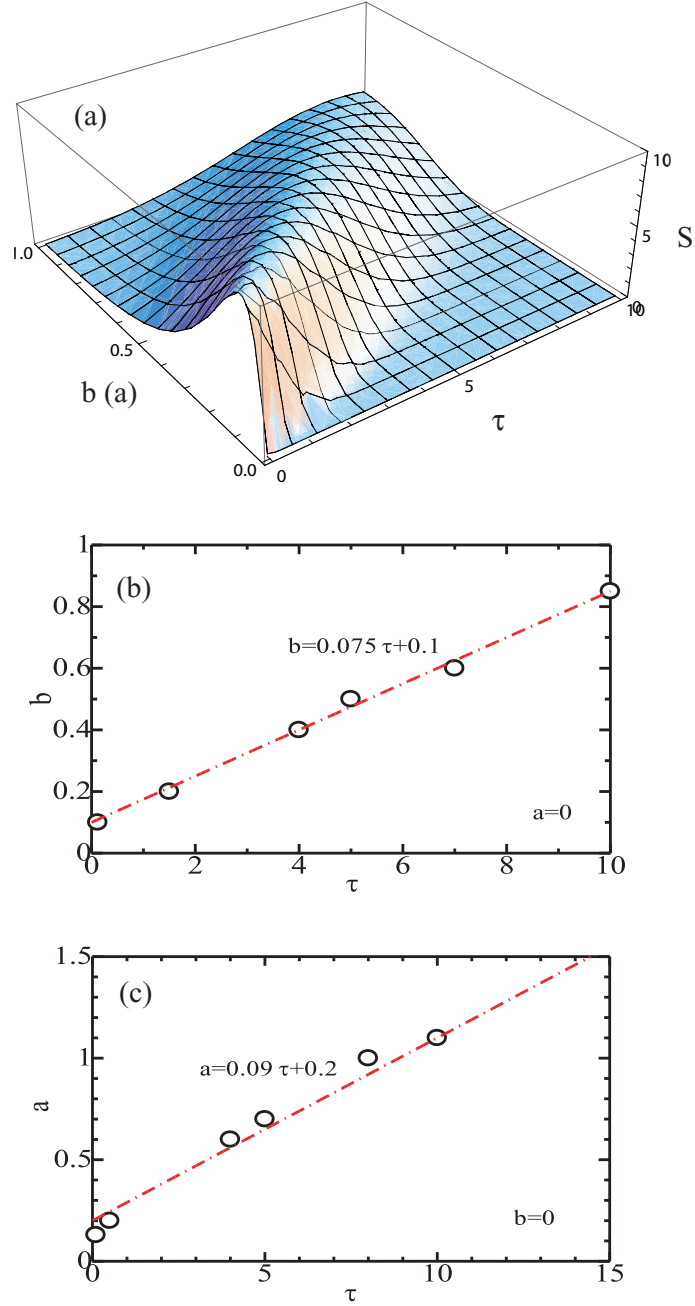


FIG. 3: (Color online) (a) A schematic plot of S as functions of b and τ (a and τ) for additive (multiplicative) noise only. (b) Locations of S_{max} for additive colored noise only in the b - τ plane obtained by simulations (circles), the chain line being expressed by $b = 0.075\tau + 0.1$. (c) Locations of S_{max} for multiplicative colored noise only in the a - τ plane obtained by simulations (circles), the chain line being expressed by $a = 0.09\tau + 0.2$.

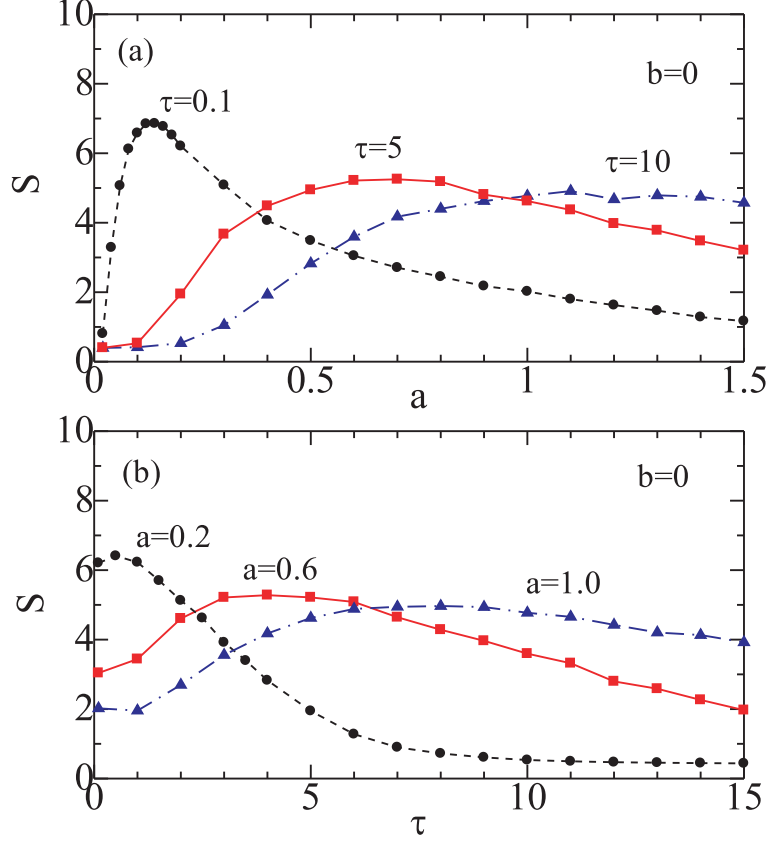


FIG. 4: (Color online) (a) SPA S for multiplicative colored noise only as a function of a with $\tau = 0.1$ (dashed curve), $\tau = 5.0$ (solid curve) and $\tau = 10.0$ (chain curve). (b) S as a function of τ with $a = 0.2$ (dashed curve), $a = 0.6$ (solid curve) and $a = 1.0$ (chain curve) ($b = 0.0$, $g = 0.05$ and $T_0 = 10.0$).

3. Case of multiplicative colored noise only

Figure 4(a) shows the a dependence of S when we apply only multiplicative colored noise with $\tau = 0.1$ (dashed curve), $\tau = 5.0$ (solid curve) and $\tau = 10.0$ (dashed curve). With increasing τ , the S_{max} value is moved to a larger a and S_{max} is gradually decreased. Figure 4(b) shows the τ dependence of S calculated for $a = 0.2$ (dashed curve), $a = 0.6$ (solid curve) and $a = 1.0$ (dashed curve).

We expect from simulation results in Figs. 4(a) and 4(b) that the a - and τ -dependent PSA is given by Fig. 3(a) where we read the b axis as the a axis. As in the case where only additive colored noise is added, a location of S_{max} departs from the origin of $(a, \tau) = (0.0, 0.0)$ and its magnitude is gradually decreased with increasing a or τ . Circles in Fig. 6(c) denote

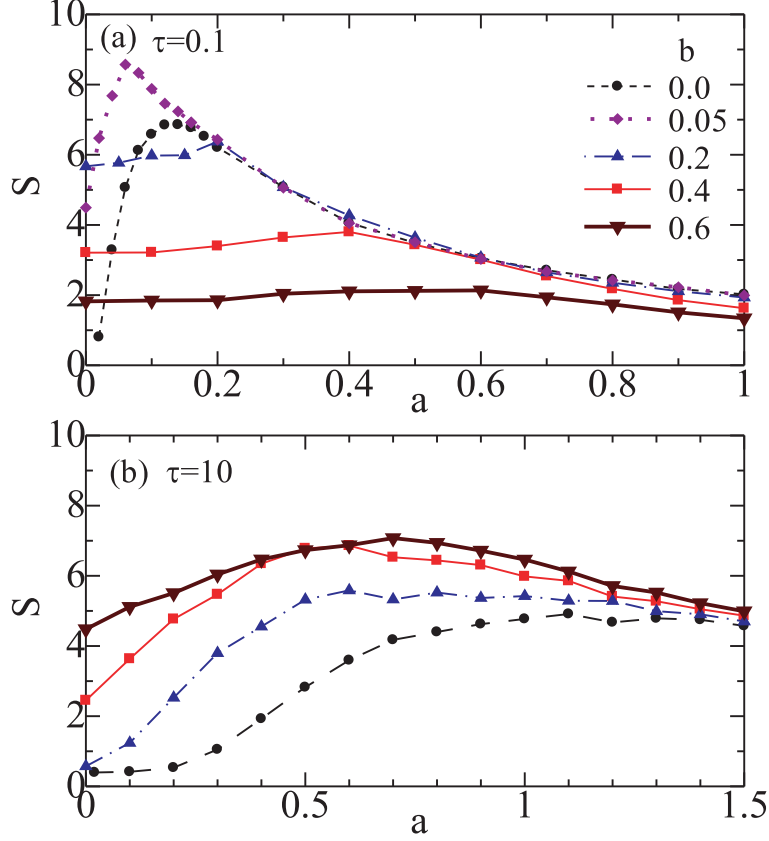


FIG. 5: (Color online) SPA S for coexisting additive and multiplicative colored noises with (a) $\tau = 0.1$ and (b) $\tau = 10.0$: $b = 0.0$ (dashed curves), $b = 0.05$ (dotted curves), $b = 0.2$ (chain curves), $b = 0.4$ (solid curves), and $b = 0.6$ (bold solid curve) ($g = 0.05$ and $T_0 = 10.0$).

locations of S_{max} in the a - τ plane obtained by simulations shown in Figs. 4(a) and (b). S_{max} nearly locates along the chain curve expressed by $a = 0.09\tau + 0.2$.

4. Case of coexisting additive and multiplicative colored noises

Next we study the case where both additive and multiplicative colored noises coexist. Figure 5(a) shows the a dependence of S for $\tau = 0.1$ with $b = 0.0$ (dashed curves), $b = 0.05$ (dotted curve), $b = 0.2$ (chain curves) and $b = 0.4$ (solid curves). The dashed curve for $b = 0.0$ shows that S has the maximum at $a \simeq 0.14$, as having been shown in Fig. 4(a). With adding small additive noise of $b = 0.05$, S_{max} is increased and its location moves to a smaller value of $a \simeq 0.05$. With further increase of b (≥ 0.2), however, the magnitude of S is gradually decreased and its maximum becomes obscure. Figure 5(b) shows the similar a

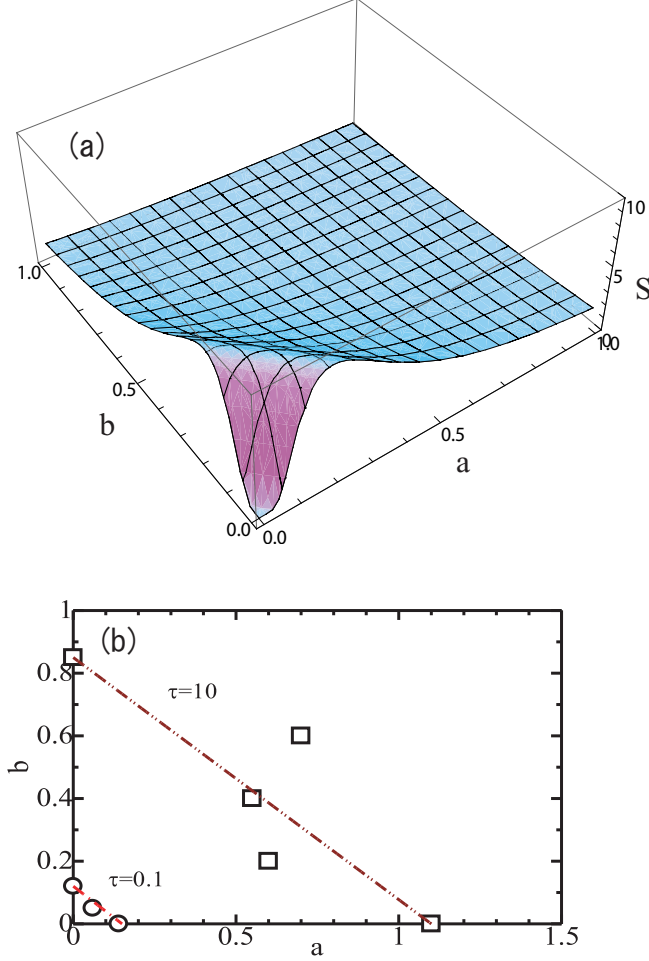


FIG. 6: (Color online) (a) A schematic plot of S as functions of a and b for coexisting additive and multiplicative noises. (b) Locations of S_{max} in the a - b plane: circles and squares denote S_{max} for $\tau = 0.1$ and $\tau = 10.0$, respectively, obtained by simulations, chain and double-chain curves being shown for a guide of the eye.

dependence of S for $\tau = 10.0$. With introducing additive noise, S is monotonously decreased.

Figure 6(a) expresses a schematic plot of S as functions of a and b for the case of coexisting additive and multiplicative noises, which are estimated from results of simulations shown in Figs. 5(a) and 5(b). S has a small value at the origin of $(a, b) = (0.0, 0.0)$. With departing from the origin by increases of a and/or b , S is first increased and then decreased after passing the maximum. Circles and squares in Fig. 6(b) denote locations of S_{max} in the a - b plane obtained from Figs. 5(a) and (b). S_{max} nearly locates along a chain (double-chain) curve for $\tau = 0.1$ ($\tau = 10.0$): in the case of $\tau = 10.0$ locations of S_{max} are scattered because

its maximum is obscure [Fig. 5(b)].

IV. DISCUSSION

A. Overdamped Langevin equation

We will derive the overdamped Langevin equation from the Markovian Langevin model given by Eq. (28). The overdamped limit of the Markovian Langevin equation is conventionally derived with setting $\ddot{x} = 0$ in Eq. (28). This is, however, not the case because dissipation and diffusion terms are state dependent in Eq. (28). Sancho, San Miguel and Dürr [35] have developed an adiabatic elimination procedure to obtain an exact overdamped Langevin equation and its FPE. In order to adopt their method [35], we rewrite Eq. (28) as

$$\ddot{x}(t) = -V'(x(t)) - \lambda(x(t))\dot{x}(t) + g(x(t))\xi(t) + f(t), \quad (40)$$

with

$$\lambda(x) = \gamma_0 \phi'(x)^2, \quad (41)$$

$$g(x) = \sqrt{2k_B T \gamma_0} \phi'(x). \quad (42)$$

By the adiabatic elimination in Eq. (40) after Ref. [35], the FPE in the Stratonovich interpretation is given by

$$\frac{\partial P(x, t)}{\partial t} = \frac{\partial}{\partial x} \frac{1}{\lambda(x)} \left[V'(x) - f(t) + k_B T \frac{\partial}{\partial x} \right] P(x, t), \quad (43)$$

where we employ the relation: $g(x)^2 = 2k_B T \lambda(x)$ derived from Eqs. (41) and (42). The relevant Langevin equation is given by [35]

$$\dot{x} = -\frac{[V'(x) - f(t)]}{\lambda(x)} - \frac{1}{2\lambda(x)^2} g'(x)g(x) + \frac{g(x)}{\lambda(x)} \xi(t). \quad (44)$$

Note that the second term of Eq. (44) does not appear when we obtain the overdamped Langevin equation by simply setting $\ddot{x} = 0$ in Eq. (40). It is easy to see that the stationary distribution of Eq. (43) with $f(t) = 0$ is given by

$$P(x) \propto e^{-\beta V(x)}. \quad (45)$$

In the case of $\phi(x) = ax^2/2 + bx$ and $f(t) = 0$, Eqs. (41), (42) and (44) lead to the overdamped Langevin equation subjected to additive and multiplicative noises given by

$$\dot{x} = -\frac{V'(x)}{\gamma_0(b+ax)^2} - \frac{k_B T a}{\gamma_0(b+ax)^3} + \sqrt{\frac{2k_B T}{\gamma_0(b+ax)^2}} \xi(t). \quad (46)$$

Equation (46) is quite different from a widely-adopted phenomenological Langevin model given by

$$\dot{x} = -V'(x) + \sqrt{2D} \xi(t) + \sqrt{2M} x \eta(t) + f(t), \quad (47)$$

with $\langle \xi(t)\xi(t') \rangle = \delta(t-t')$ and $\langle \eta(t)\eta(t') \rangle = \delta(t-t')$. The stationary PDF obtained from the PFE for Eq. (47) in the Stratonovich sense is given by

$$\ln P(x) = -\int \frac{V'(x)}{(D+Mx^2)} dx - \left(\frac{1}{2}\right) \ln(D+Mx^2). \quad (48)$$

For the parabolic potential of $V(x) = x^2/2$, Eq. (48) yields Gaussian or non-Gaussian PDF, depending on D and M [28–30]. For the bistable potential of $V(x) = x^4/4 - x^2/2$, Eq. (48) leads to

$$P(x) \propto (D+Mx^2)^{-(M^2-M-D)/2M^2} e^{-x^2/2M} \quad \text{for } D \neq 0.0, M \neq 0.0, \quad (49)$$

$$\propto e^{-(x^4/4-x^2/2)/D} \quad \text{for } M = 0.0, \quad (50)$$

$$\propto |x|^{1/M-1} e^{-x^2/2M} \quad \text{for } D = 0.0. \quad (51)$$

Stationary PDF of Eq. (48) depends on D and M in contrast with that of Eq. (45) which is independent of them.

B. The CL model with two kinds of noises

The CL-type system-bath model in which the system is driven by two kinds of noises has been proposed. Assuming that a bath is driven by an external noise, Ref. [36] has adopted the Hamiltonian given by Eqs. (8)-(10) but $H_B + H_I$ in Eq. (10) is replaced by

$$H_B + H_I = \sum_{n=1}^N \left\{ \frac{p_n^2}{2m_n} + \frac{m_n \omega_n^2}{2} \left(q_n - \frac{c_n \phi(x)}{m_n \omega_n^2} \right)^2 + \kappa_n q_n \epsilon(t) \right\}. \quad (52)$$

where $\epsilon(t)$ denotes an external noise with zero mean and correlation function,

$$\langle \epsilon(t) \rangle_e = 0, \quad \langle \epsilon(t)\epsilon(t') \rangle_e = 2D_e \Psi(t-t'), \quad (53)$$

D_e is the external noise strength, $\Psi(t - t')$ is the external noise kernel, κ_n expresses the bath-noise coupling, and $\langle \cdot \rangle_e$ implies an average over the external noise process. Eliminating bath variables in a conventional way, we obtain the Langevin equation given by [36]

$$\begin{aligned} \ddot{x}(t) = & -V'(x(t)) - \phi'(x(t)) \int_0^t \gamma(t - t') \phi'(x(t')) \dot{x}(t') dt' + \phi'(x(t)) [\zeta(t) + \pi(t)] \\ & + f(t), \end{aligned} \quad (54)$$

where $\gamma(t)$ and $\zeta(t)$ are given by Eqs. (12) and (13), respectively, and $\pi(t)$ is expressed by

$$\pi(t) = - \int_0^\infty \psi(t - t') \epsilon(t') dt', \quad (55)$$

with

$$\psi(t) = \sum_{n=1}^N \frac{c_n \kappa_n \sin \omega_n t}{m_n \omega_n}. \quad (56)$$

Equation (54) indicates that the system is driven by two kinds of noises, $\zeta(t)$ and $\pi(t)$, both of which are multiplicative with the same functional form of $\phi'(x(t))$. The correlation of an effective noise $\tilde{\zeta}(t) [= \zeta(t) + \pi(t)]$ becomes [36]

$$\langle \langle \tilde{\zeta}(t) \tilde{\zeta}(t') \rangle \rangle_e = k_B T \gamma(t - t') + 2D_e \int_0^t \int_0^{t'} \psi(t - t'') \psi(t' - t''') \Psi(t'' - t''') dt'' dt''', \quad (57)$$

which is similar to but different from the FDR given by Eq. (14). We note that although the Markovian limit of Eq. (54) given by

$$\ddot{x}(t) = -V'(x(t)) - \gamma_0 \phi'(x(t))^2 \dot{x}(t) + \phi'(x(t)) [\zeta(t) + \pi(t)] + f(t), \quad (58)$$

resembles the Langevin model given by Eq. (4), we cannot regard the former as a microscopic counterpart of the latter because the external noise $\epsilon(t)$ introduced in Eq. (52) is phenomenological and the FDR does not hold in Eq. (54).

V. CONCLUSION

We have studied an open bistable system subjected to additive and multiplicative colored noises which is described by the generalized CL model [18–20, 27]. Our microscopic model in which the FDR is preserved goes beyond the deficits (a)-(c) in the phenomenological Langevin model mentioned in Sec. I. Calculated results for an open bistable system are summarized as follows:

(i) marginal PDFs for x and p are given by $P(x) \propto e^{-\beta V(x)}$ and $P(p) \propto e^{-\beta p^2/2}$, respectively, independently of noise parameters of a , b and τ (Fig. 1) although SPA depends on them,

(ii) calculated SPA exhibits SR for a variation of τ [Figs. 2(b) and 4(b)] besides of a and b [Figs. 2(a) and 4(a)], and

(iii) SPA for coexisting additive and multiplicative noises shows unimodal but bimodal structures as functions of a , b and/or τ [Figs. 3(a) and 6(a)].

Items (i)-(iii) are in contrast with the results obtained by the phenomenological Langevin model [4–8, 10–12] where the stationary PDF depends on noise parameters, SPA shows a monotonous change with increasing τ , and SPA may exhibit the two-peak structure for coexisting additive and multiplicative noises. These differences are expected to arise from the fact that the FDR holds in our microscopic CL model but in the phenomenological Langevin model. It would be interesting to apply the present approach to a study of relevant phenomena in bistable systems such as the first passage time and resonant activation.

Acknowledgments

This work is partly supported by a Grant-in-Aid for Scientific Research from Ministry of Education, Culture, Sports, Science and Technology of Japan.

-
- [1] R. Benzi, A. Sutera, and A. Vulpiani, *J. Phys. A* **14**, L453 (1981); R. Benzi, G. Parisi, A. Sutera, and A. Vulpiani, *Tellus* **34**, 10 (1982).
 - [2] L. Gammaitoni, P. Hänggi, P. Jung, and F. Marchesoni, *Rev. Mod. Phys.* **70**, 223 (1998).
 - [3] B. Lindner, J. Garcia-Ojalvo, A. Neiman, and L. Schimansky-Geilier, *Phys. Rep.* **392**, 321 (2004).
 - [4] C. Li, W. Da-ji, and K. Shen-zhi, *Phys. Rev. E* **52**, 3228 (1995).
 - [5] Hai-Xiang Fu, Li Cao and Da-Jin Wu, *Phys. Rev. E* **59**, R6235 (1999).
 - [6] P. Hänggi, F. Marchesoni, and P. Grigolini, *Z. Phys. B* **56**, 333.
 - [7] P. Hänggi, P. Jung, C. Zerbe, and F. Moss, 1993, *J. Stat. Phys.* **70**, 25 (1993).
 - [8] P. Hänggi, and P. Jung, *Adv. Chem. Phys.* **89**, 239 (1995).
 - [9] P. Jung and P. Hänggi, *Phys. Rev. A* **35**, 4464 (1987).

- [10] Ya Jia, S. N. Yu, and J. R. Li, Phys. Rev. E **62**, 1869 (2000).
- [11] Ya Jia, Xiao-ping Zheng, Xiang-ming Hu, and Jia-rong Li, Phys. Rev. E **63**, 031107 (2001).
- [12] Xiaoqin Luo and Shiqun Zhu, Phys. Rev. E **67**, 021104 (2003).
- [13] G. W. Ford, M. Kac and P. Mazur, J. Math. Phys. **6**, 504 (1965).
- [14] P. Ullersma, Physica **32**, 27 (1966); *ibid.* **32**, 56 (1966); *ibid.* **32**, 74 (1966); *ibid.* **32**, 90 (1966).
- [15] A. O. Caldeira and A. J. Leggett, Phys. Rev. Lett. **46**, 211 (1981); A. O. Caldeira and A. J. Leggett, Ann. Phys. **149**, 374 (1983).
- [16] K. Lindenberg and V. Seshadri, Physica A **109**, 483 (1981); K. Lindenberg and E. Cortés, *ibid.* **126**, 489 (1984).
- [17] E. Pollak and A. M. Berezhkovskii, J. Chem. Phys. **99**, 1344 (1993).
- [18] D. Barik and D. S. Ray, J. Stat. Phys. **120**, 339 (2005).
- [19] A. V. Plyukhin and A. M. Froese, Phys. Rev. E **76**, 031121 (2007).
- [20] R. L. S. Farias, Rudnei O. Ramos, and L. A. da Silva, Phys. Rev. E **80**, 031143 (2009).
- [21] S. Zaitsev, O. Shtempluck and E. Buks, arXiv:0911.0833.
- [22] A. Eichler, J. Moser, J. Chaste, M. Zdrojek, I. Wilson-Rae, and A. Bachtold, arXiv:1103.1788.
- [23] M. O. Magnasco, Phys. Rev. Lett. **71**, 1477 (1993).
- [24] F. Jülicher, A. Ajdari, and J. Prost, Rev. Mod. Phys. **69**, 1269 (1997).
- [25] P. Reimann, Phys. Repts. **361**, 57 (2002).
- [26] M. Porto, M. Urbakh, and J. Klafter, Phys. Rev. Lett. **85**, 491 (2000); G. Oshanin, J. Klafter, M. Urbakh, and M. Porto, Europhys. Lett. **68**, 26 (2004).
- [27] H. Hasegawa, Phys. Rev. E **84**, 051124 (2011): Eq. (38) of this reference is erroneous and it should be Eq. (31) in this paper.
- [28] H. Sakaguchi, J. Phys. Soc. Jpn. **70**, 3247 (2001).
- [29] C. Anteneodo and C. Tsallis, J. Math. Phys. **44**, 5194 (2003).
- [30] H. Hasegawa, Physica A **374**, 585 (2007).
- [31] A. Timmermann and G. Lohmann, J. Phys. Oceanogr. **32**, 1112 (2001).
- [32] H. Hasegawa, Physical A **384**, 241 (2007).
- [33] In the Heun method for the ordinary differential equation of $dx/dt = f(x)$, a value of x at $t+h$ is evaluated by $x(t+h) = x(t) + (h/2)[f(x_0) + f(x_1)]$ with $x_0 = x(t)$ and $x_1 = x(t) + hf(x(t))$, while it is given by $x(t+h) = x(t) + hf(x(t))$ in the Euler method, h being the time step. The Heun method for the stochastic ordinary differential equation meets the Stratonovich

calculus employed in the FPE [34].

- [34] W. Rümelin, SIAM J. Numer. Anal. **19**, 604 (1982); A. Greiner, W. Strittmatter, and J. Honerkamp, J. Stat. Phys. **51** 95 (1988); R.F. Fox, I.R. Gatland, R. Roy, and G. Vemuri, Phys. Rev. A **38** 5938 (1988).
- [35] J. M. Sancho, M. San Miguel, and D. Dürr, J. Stat. Phys. **28**, 291 (1982).
- [36] J. R. Chaudhuri, S. K. Banik, B. C. Bag, and D. S. Ray, Phys. Rev E **63**, 061111 (2001).